Pollution 2022, 8(2): 397-406
DOI: 10.22059/POLL.2021.324884.1107

RESEARCH PAPER

Removal of Iron from Aqueous Solution by using *Typha australis* Leaves as Low Cost Adsorbent

Fatimetou Mohamed N'Dah[1], **Mohamed Sid'Ahmed Kankou**[1], **Mohamed Abdallahi Bollahi** [2] and **Abdoulaye Demba N'diaye** [1,*]

1. Unité de Recherche Eau, Pollution et Environnement, Département de Chimie, Faculté des Sciences et Technique, Université de Nouakchott Al Aasriya, BP 880, Nouakchott, Mauritanie
2. Laboratoire de Chimie, Service de Toxicologie et de Contrôle de Qualité, Institut National de Recherches en Santé Publique, BP 695, Nouakchott, Mauritanie

Received: 01.06.2021, Revised: 06.12.2021, Accepted: 12.12.2021

ABSTRACT

Iron removal from aqueous solution via ultrasound-assisted adsorption using *Typha australis* leaves as low cost adsorbent had been studied. The effects of various experimental parameters like mass of the *Typha australis* adsorbent and contact time have been investigated using a batch experiment. The adsorption kinetic data were analyzed using the Pseudo First Order (PFO) and Pseudo Second Order (PSO) models. The adsorption modeling was carried out using the Langmuir, Freundlich and Redlich-Peterson adsorption models. For kinetic study, the adsorption process fitted the PSO model and agreed with chemisorption. Both the Langmuir and Redlich–Peterson models were found to fit the adsorption isotherm data well, but the Redlich– Peterson model was better. The maximum adsorption capacity from the Langmuir model (q_{max}) was 0.84 mg/g. The results of the present work showed that the *Typha australis* leaf, without any treatment has a good potential for iron removal from aqueous solutions via ultrasound-assisted adsorption.

Keywords: ultrasound-assisted adsorption, nonlinear method, kinetics, isotherms.

INTRODUCTION

Heavy metal pollution is one of the major perils to the environment (Islam et al., 2015). Among the heavy metals, iron is one of the earth's most abundant elements. Iron deficiency is the most common nutritional deficiency causing anemia (Miller, 2013). The iron toxicity may lead to various diseases like liver damage, hypothermia, etc. The presence of iron in aquatic media causes aesthetic and organoleptic problems (Inglezakisa et al., 2010).

Some techniques have been developed for the removal of metals from water like chemical precipitation and ion exchange (Izadi et al., 2017), chemical and electrocoagulation (Martín-Domínguez et al., 2018), solvent extraction (Wang et al., 2020), electrochemical (Rosa et al., 2017), bioelectrochamical (Sukrampal et al., 2020), biological operations (Gopi Kiran et al., 2017), filtration (Almasian et al., 2018), membrane processes (Tian et al., 2020) and adsorption (Zhang et al., 2020). However, adsorption is one of the most widely applied techniques for iron and other pollutants removal. In addition, the activated carbon is cost-prohibitive.

For these reasons, researchers have concentrated on finding alternative natural adsorbents to activated carbon. Natural adsorbents are preferred for their biodegradable, non-toxic nature, low commercial value and highly cost-effective nature.

* Corresponding author Email: abdouldemba@yahoo.fr

In this work, *Typha australis,* an abundant and available plant along the Senegal River, was chosen to investigate its adsorption capacity for iron present in aqueous solution using the ultrasound assisted batch operation. Insofar as, many authors have reported that the innovative technologies used in combination with adsorption is sonication (Zare- Dorabei et al., 2016). The effects of *Typha australis* leaf adsorbent mass and contact time on the adsorption efficiency of iron were studied using the batch experiment. The kinetics of iron adsorption on *Typha australis* leaves adsorbent was analyzed by Pseudo First Order (PFO) and Pseudo Second Order (PSO) kinetic models. Experimental equilibrium data were fitted to the Langmuir, Freundlich and Redlich-Peterson isotherm models.

MATERIAL AND METHODS

A stock solution containing 1,000 mg/L of iron was purchased. Iron solutions were prepared by diluting stock solution of iron to the desired concentrations in distilled water. The concentrations of iron in the solutions before and after adsorption were determined using an Atomic Absorption Spectroscopy PGG 990.

Biomass of *Typha australis* growing along the Senegal River was collected from Mauritania. The collected biomass was prepared according to N'diaye et al, (2020_a). Fourier transform infrared (FTIR) spectra of *Typha australis* leaves adsorbent before and after iron adsorption were recorded, in the range of 4000 to 500 cm^{-1}, using an FTIR 650 (Lab Kits)

Batch experiments were carried out by varying several experimental variables such as *Typha australis* leaves adsorbent dosage (0.1-3 g) and contact time (10–120 min). The adsorption isotherms were obtained by varying the initial iron concentrations from 1 to 50 mg/ L. In all sets of experiments were sonicated by ultrasonic bath Fisherbrand FB15050 at pH 6.8. The concentrations of iron in the solutions before and after adsorption were determined using an Atomic Absorption Spectroscopy PGG 990. At the end of each experiment, the sonicated solution mixture was micofiltered and the residual concentration of iron was determined. The adsorption uptake at equilibrium time, q_e, and the percentage of the removal R (%) was expressed by equations (1) and (2), respectively:

$$q_e = \frac{(C_i - C_e)V}{m} \tag{1}$$

$$\text{R (\%)} = \frac{C_i - C_e}{C_i} \times 100 \tag{2}$$

Where q_e is the amount of iron adsorbed by *Typha australis* leaves adsorbent (mg/g), C_i is the initial iron concentration (mg/L), C_e is the iron concentration at equilibrium (mg/L), V is the solution volume (L) and m is the mass of *Typha australis* leaves adsorbent used (g).

To estimate the adsorption mechanism can be considered as a physical or chemical mechanism, PFO and PSO models were applied to investigate the adsorption data (HO, 2006). The nonlinear kinetics PFO and PSO models may be expressed by (3) and (4), respectively:

$$q_t = q_e(1 - \exp^{-k_1 t}) \tag{3}$$

$$q_t = \frac{k_2 q_e^2 t}{1 + k_2 q_e t} \tag{4}$$

Where q_t is the amount of iron adsorbed per unit mass of *Typha australis* leaves adsorbent (mg/g) at time t, k_1 (L/min) is the PFO rate constant, k_2 (mg/g min) is the PSO rate constant for adsorption, q_e (mg/g) the amount of iron adsorbed at equilibrium and t is the contact time (min).

Langmuir, Freundlich and Redlich-Peterson adsorption isotherms were used to analyze the adsorption isotherms of iron. The Langmuir adsorption isotherm model assumed that adsorption takes place at specific homogeneous sites within the adsorbent. The Langmuir equations are expressed by the following relation (Langmuir, 1918):

$$q_e = \frac{q_m K_L C_e}{1 + K_L\, C_e} \tag{5}$$

Where q_e is the amount of iron adsorbed per unit mass of *Typha australis* leaves adsorbent (mg/g), k_L is the Langmuir constant related to the adsorption capacity (L/g), C_e is the concentration of iron in the solution at equilibrium (mg/L), q_m is the maximum uptake per unit mass of *Typha australis* leaves adsorbent (mg/g). The factor of separation of Langmuir, R_L is calculated by equation (6):

$$R_L = \frac{1}{(1 + k_L C_0)} \tag{6}$$

Where C_0 is the higher initial concentration of iron and K_L is the Langmuir constant. The R_L value implies the adsorption to be defavourable (R_L>1), linear (R_L=1), favourable (0<R_L<1), or irreversible (R_L=0).

The Freundlich adsorption isotherm model considers a heterogeneous adsorption surface that has unequal available sites with different energies of adsorption. The Freundlich adsorption isotherm model is represented as follow (Freundlich, 1959):

$$q_e = K_F C_e^{1/n} \tag{7}$$

Where K_F (mg/g) (L/mg) ^{n} and 1/n are the Freundlich constants related to adsorption capacity and adsorption intensity, respectively.

The Redlich–Peterson isotherm model combines the Langmuir and Freundlich models and the mechanism of adsorption is a hybrid one (Redlich-Peterson, 1959). The nonlinear representation of the Redlich–Peterson model is as in equation (8):

$$q_e = \frac{K_{RP} C_e}{1 + \alpha_{RP} C_e^n}$$

(8)

Where K_{RP} (L/g) and α_{RP} (L/mol) are the Redlich-Peterson isotherm constants, while n is the exponent, which lies between 0 and 1. The correlation coefficient (R^2) values, by using the Solver Excel, are determined by following equation (9):

$$R^2 = 100\left(1 - \frac{\left\| q_{exp} - q_{mod} \right\|^2}{\left\| q_{exp} - q_{avr} \right\|^2}\right) \tag{9}$$

Where q_{exp} (mg/g) is equilibrium capacity from the experimental data, q_{avr} (mg/g) is equilibrium average capacity from the experimental data and q_{mod} (mg/g) is equilibrium from model. So that $R^2 \leq 100$ – the closer the value is to 100, the more perfect is the fit.

RESULTS AND DISCUSSION

The results of the physical and chemical analysis showed pHpzc of 6.4, a moisture content of 3.9 %, total surface acidity of 0.744 meq/g, total surface basicity of 0.376 meq/g and BET surface of 0.91 m^2/g (N'diaye et al., 2020_a). The quantification of the *Typha australis* adsorbent by Boehm titration reveals that the adsorbent has also the greatest content of acidic surface than the basic surface groups. The surface of the present study is comparable to that found by Barrera-Diaz et al., (2010) who reported a surface area of 0.84 m^2/g of *Typha latifolia*. The value of the surface area of *Typha australis* without any thermal or chemical process is satisfactory when compared with other species of Typha studied in the literature whose preparations required excessive heat and chemical inputs and especially with the use of toxic acids and corrosive. The outcome of the ultimate elemental analysis of *Typha australis* leaves indicates that Oxygen (49.04 %) and Carbon (43.93 %) are the major constituents of *Typha australis* leaves along with the quantifiable amount of Hydrogen (5.87 %), Nitrogen (0.88 %) and Sulfur (0.28 %). We also observe that *Typha australis* contains only 0.88 % Nitrogen and 0.28 % Sulfur. This is consistent with the fact that the main constituents of *Typha australis* are cellulose and lignin (N'diaye et al., 2020_b).

Fig. 1 shows FTIR spectra of the *Typha australis* leaves adsorbent before and after iron adsorption. The result of the FTIR study of *Typha australis* leaves adsorbent showed absorption peaks located 3853, 3750, 3567, 2921, 2358, 1652, 1449 and 605 cm^{-1} (Fig.1). The small peak observed at 2921 cm^{-1} denotes the presence of the stretching C–H vibration in the quinine group. Peak at 1652 cm^{-1} are assigned to C=O (amide band/ OH). The absorption peak at 1449 cm^{-1} can be attributed to the presence of (CH_2 and CH_3). After iron adsorption, the slight shift of peaks was at 3750, 3735, 2913, 2362, 1654, 1449 and 593 cm^{-1} (Fig.1).

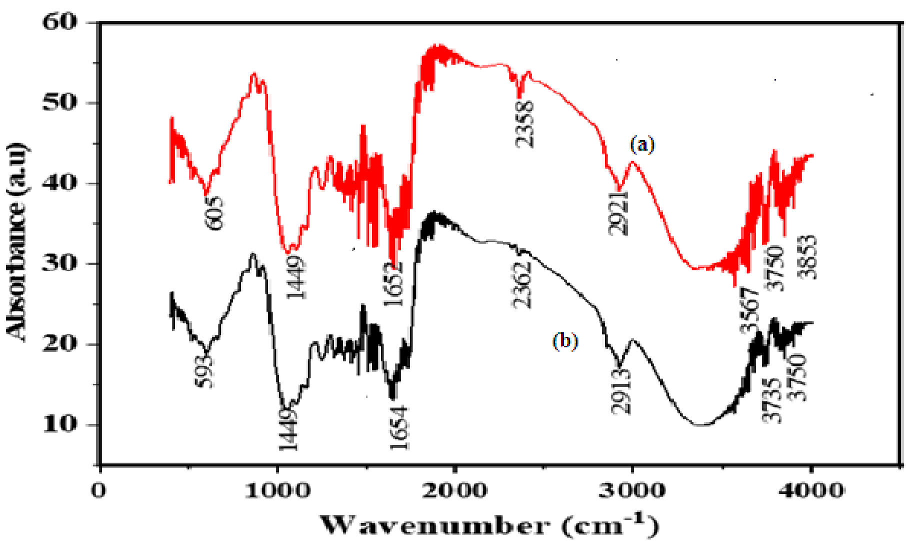

Fig. 1: FTIR spectra of Typha australis leaves adsorbent before (a) and after (b) Iron adsorption

The changes observed in the FTIR spectrum reflects the evidence for the interaction between iron ion and the functional groups present on the surface of the *Typha australis* adsorbent that might be involved in the adsorption process of the metal. Moreover, it could be seen that there was a slight shift of absorption peaks, but the intensity do not change after adsorption, which indicated a chemical adsorption.

Variation of mass in the range 0.1–3 g at a fixed iron concentration (1 mg/L) for iron removal by *Typha australis* leaves is shown in Fig. 2. The results suggest that the increase in the mass of *Typha australis* leaves adsorbent results in an increase in adsorption. The percentage iron removal increases from 30.5 to 61 % when *Typha australis* leaves adsorbent dose is increased from 0.1 to 0.5 g in case of initial solution concentration of 1 mg/L. It is observed that the % removals of iron increased as the dose of *Typha australis* leaves adsorbent increased. About 0.5 g the % removal of iron increases slightly to 1 g to reach equilibrium. According to (Nair et al., 2014), this may be attributed to the increased adsorbent surface area, pores, active sites and the number of unsaturated sites. Finally, in the rest of the work for to determine the kinetic models and adsorption isotherms we have chosen 0.5 g of *Typha australis* leaves doses.

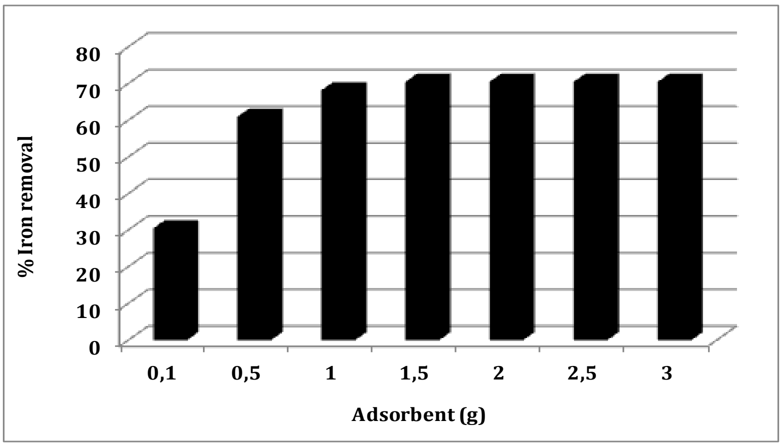

Fig. 2: Effect of Typha australis leaves dosage on Iron removal percentage

The effect of contact time on removal of iron (1 and 5 mg/L) is shown in Fig. 3. The results showed that the removal of iron by adsorption on *Typha australis* leaves adsorbent was found to be rapid at the initial period of contact and then to slow down with increasing in contact time. At equilibrium, 69 and 43 % for 1 and 5 mg/L respectively are obtained with a contact time of 60 min for *Typha australis* leaves adsorbent which is shown in Fig. 3. The same results were reported by other investigators (Adekola et al., 2016; Kwakye-Awuah et al., 2019).

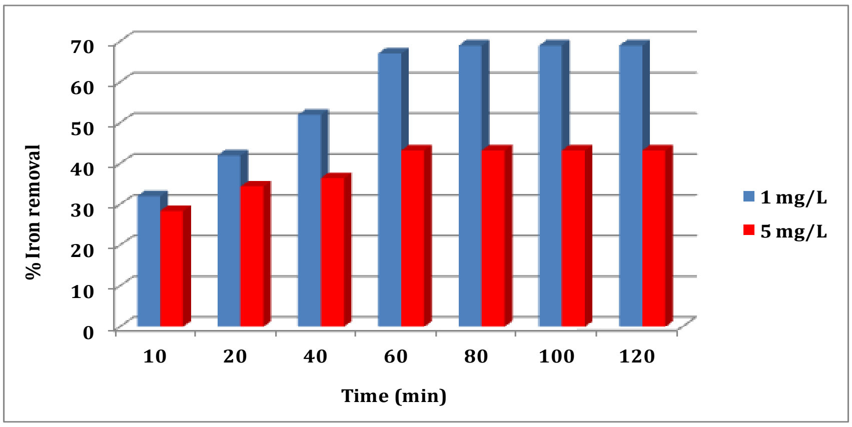

Fig. 3: Effect of contact time on the removal of Iron by Typha australis leaves adsorbent

Figs. 4-5 show the experimental data and the predicted theoretical kinetics for the adsorption of iron onto *Typha australis* leaves adsorbent for 1 and 5 mg/L. The values of model parameters q_e, k_1, k_2 and R^2 are presented in Table 1.

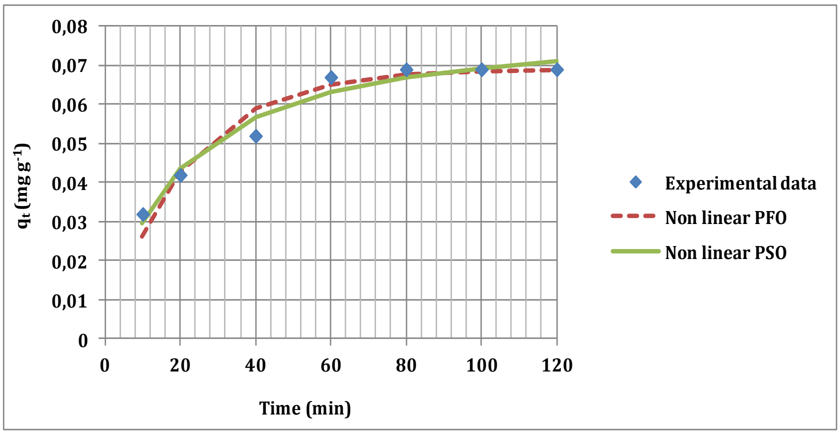

Fig. 4: PFO and PSO non linear by Typha australis leaves adsorbent with initial Iron concentration of 1 mg/L

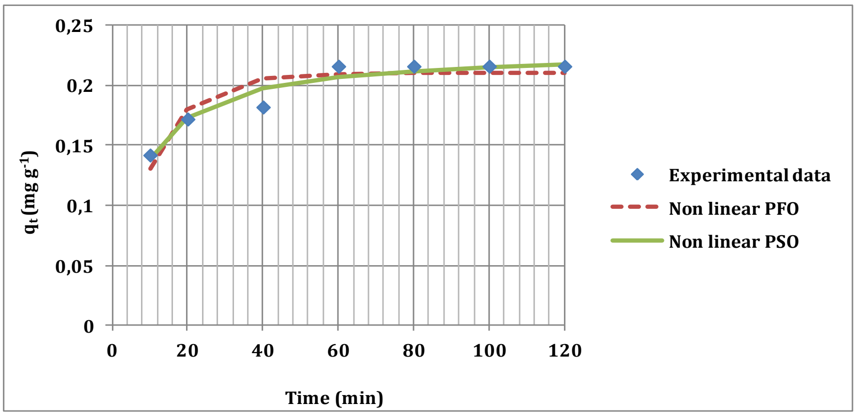

Fig. 5: PFO and PSO non linear by Typha australis leaves adsorbent with initial Iron concentration of 5 mg/L

Table 1: PFO and PSO models constants and R^2 for the adsorption of Iron by *Typha australis* leaves adsorbent

Model	Parameters	1 mg /L	5 mg /L
	q_{exp}	0.069	0.216
PFO	q_e	0.069	0.210
	K_1	0.048	0.097

	R^2 (%)	93.9	82.8
	q_e	0.081	0.226
PSO	K_2	0.71	0.66
	R^2 (%)	96.2	93.5

These results demonstrate that PSO model displays more satisfactory correlation for the adsorption of iron, suggesting that the adsorption process was predominantly controlled by chemical reactions between the iron and the adsorption sites of the *Typha australis* leaves adsorbent. Similar results are reported by other authors (Nagel-Hassemer et al., 2013).

Fig. 6 show the experimental data fitted to non-linear forms of the three isotherms for iron adsorption by *Typha australis* leaves adsorbent. The isotherms constants related to Langmuir, Freundlich and Redlich-Peterson models determined from the plots shown in Fig. 6 are listed in Table 2.

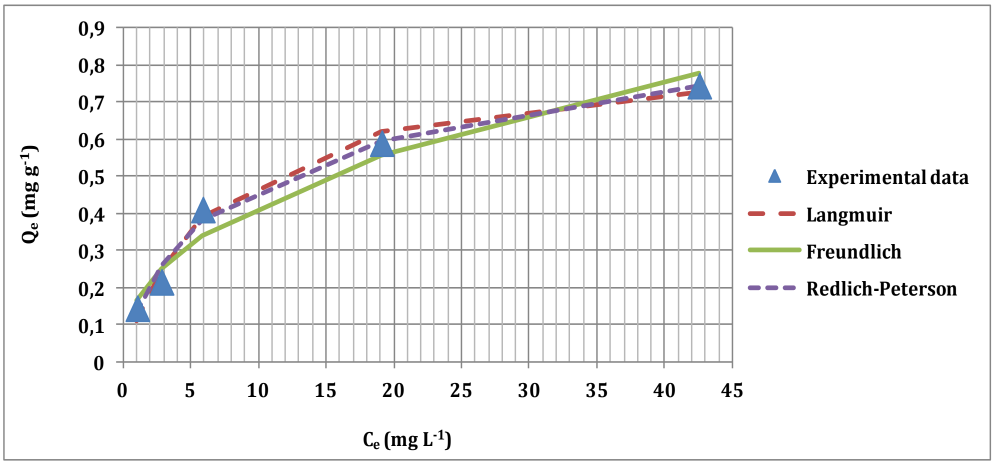

Fig. 6: Comparison between the experimental and predicted isotherms for the adsorption of Iron by Typha australis leaves adsorbent

Table 2: Parameters of the Langmuir, Freundlich and Redlich-Peterson isotherms of Iron by Typha australis leaves adsorbent

Model	Parameters	Value
Langmuir	**q_m**	0.84
	K_L	0.15
	R_L	0.12
	R^2 (%)	98.6
Freundlich	**1/n**	0.42
	K_F	0.16
	R^2 (%)	97.3
Redlich-Peterson	**K_{RP}**	0.18
	α_{RP}	0.41
	n	0.83
	R^2 (%)	99.04

From Table 2, the Redlich–Peterson and Langmuir models gave the highest R^2 values showing that the adsorption isotherms of iron by *Typha australis* leaves were best described by these two models. It was observed that both the Langmuir and Redlich-Peterson isotherms could well represent the experimental adsorption data. The suitability of the Langmuir isotherm to fit the data was confirmed by the exponent value of the Redlich-Peterson model, n, which was near to 1 confirming that the surface of *Typha australis* leaves adsorbent is homogenous for iron adsorption. The monolayer adsorption capacity, q_m, was found to be 0.84 mg/g. In addition, the values of R_L, K_L and 1/n are in between 0 and 1 indicating that the adsorption of iron by *Typha australis* leaves adsorbent is favorable.

CONCLUSION

The adsorption of iron from aqueous solutions using *Typha australis* leaves as a low cost adsorbent has been studied. The obtained results showed that the PSO model fit the experimental data well and agreed with chemisorption. The equilibrium data were analyzed using non-linear method by fitting them to the Langmuir, Freundlich and Redlich–Peterson model equations. Both the Langmuir and Redlich–Peterson isotherms represent well the experimental adsorption data. The maximum adsorption capacity was found to be 0.84 mg/g. The values of R_L, K_L and 1/n are in between zero and one. This confirms that the adsorption of iron onto *Typha australis* leaves adsorbent is favorable. It can be concluded that the natural *Typha australis* leaves, without any treatment, could be a promising adsorbent for iron removal from aqueous solution via ultrasound-assisted adsorption.

GRANT SUPPORT DETAILS

The present research did not receive any financial support.

CONFLICT OF INTEREST

The authors declare that there is not any conflict of interests regarding the publication of this manuscript. In addition, the ethical issues, including plagiarism, informed consent, misconduct, data fabrication and/ or falsification, double publication and/or submission, and redundancy has been completely observed by the authors.

LIFE SCIENCE REPORTING

No life science threat was practiced in this research.

REFERENCES

Adekola, F.A., Hodonou, D.S.S. and Adegoke, H.I. (2016). Thermodynamic and kinetic studies of biosorption of iron and manganese from aqueous medium using rice husk ash. Appl Water Sci, 6:319–330.

Almasian, A., Giahi, M., Chizari Fard, G., Dehdast, S. A. and Maleknia, L. (2018). Removal of heavy metal ions by modified PAN/PANI-nylon core-shell nanofibers membrane: Filtration performance, antifouling and regeneration behavior. Chemical Engineering Journal, 351, 1166–1178.

Barrera-Díaz C., Colín-Cruz A., Ureña-Nuñez F., Romero-Romo M. and Palomar-Pardavé M. (2010). Cr (VI) Removal from Wastewater Using Low Cost Sorbent Materials: Roots of *Typha Latifolia* and Ashes; Environmental Technology; 25, 8.

Freundlich, H.M.F.(1959). Over the adsorption in solution, J. Phys. Chem; 63, 1024-1036.

Gopi Kiran, M., Pakshirajan, K. and Das, G. (2017). A new application of anaerobic rotating biological contactor reactor for heavy metal removal under sulfate reducing condition. Chemical Engineering Journal, 321, 67–75.

Ho, Y.S. (2006). Review of second-order models for adsorption systems. J. Hazard. Mater. B., 136, 681–689.

Inglezakisa, V.J.; Doulab, M.K.; Aggelatou, V. and Zorpas, A.A. (2010). Removal of iron and manganese from underground water by use of natural minerals in batch mode treatment. Desalin. Water Treat., 18, 341–346.

Islam, M.S., M.K. Ahmed, M. Raknuzzaman, M. Habibullah -Al- Mamun, Islam M.K. (2015). Heavy metal pollution in surface water and sediment: a preliminary assessment of an urban river in a developing country, Ecol. Indicat. 48, 282–291.

Izadi, A., Mohebbi, A., Amiri, M. and Izadi, N. (2017). Removal of iron ions from industrial copper raffinate and electrowinning electrolyte solutions by chemical precipitation and ion exchange. Minerals Engineering, 113, 23–35.

Kwakye-Awuah, B., Sefa-Ntiri, B., Von-Kiti, E., Nkrumah, I. and Williams, C. (2019). Adsorptive Removal of Iron and Manganese from Groundwater Samples in Ghana by Zeolite Y Synthesized from Bauxite and Kaolin. Water, 11, 1912.

Langmuir, I.J.(1918). The adsorption of gases on planes surfaces of glass, mica and platinum. J. Am. Chem. Soc.40, 1361-1403.

Martín-Domínguez, A., Rivera-Huerta, M. L., Pérez-Castrejón, S., Garrido-Hoyos, S. E., Villegas-Mendoza, I. E., Gelover-Santiago, S. L., … and Buelna, G. (2018). Chromium removal from drinking water by redox-assisted coagulation: Chemical versus electrocoagulation. Separation and Purification Technology, 200, 266–272.

Miller, J.L. (2013). Iron deficiency anemia: a common and curable disease, Cold Spring Harbor Perspectives in Medicine 3 (7).

Moradi, E, Rahimi, R. and Safarifard, V. (2019). Sonochemically synthesized microporous metal–organic framework representing unique selectivity for detection of Fe^{3+} ions, Polyhedron, 159, 251–258.

Nagel-Hassemer, M.E., Lapolli, F. R. and Recio, M.N.L. (2013). Simultaneous adsorption of iron and manganese from aqueous solutions employing an adsorbent coal, Environmental Technology, 34:2, 275-282.

Nair, V., Panigrahy, A. and Vinu, R. (2014). Development of novel chitosan- lignincomposites for adsorption of dyes and metal ions from wastewater. Chem. Eng.J. 254, 491–502.

N'diaye, A.D., Aoulad El Hadj Ali, Y., Bollahi, M.A., Stitou, M., Kankou M.S.A. and Fahmi D. (2020_a). Adsorption of Methylene Blue from aqueous solution using Senegal River *Typha australis.* Mediteranean Journal of Chemisty, 10 (1), 22-32.

N'diaye, A.D., Aoulad El Hadj Ali Y., El Moustapha Abdallahi, O., Bollahi, M.A., Stitou, M., Kankou, M., Fahmi, D. (2020_b). Sorption of Malachite Green from aqueous solution using *Typha australis* leaves as a low cost sorbent. Journal of Environmental Treatment Techniques, 8, 3, 1023-1028.

Redlich, O. and Peterson, D.L.(1959). A Useful Adsorption Isotherm; J. Phys. Chem. 63, 6, 1024.

Rosa, M. A., Egido, J. A. and Márquez, M. C. (2017). Enhanced electrochemical removal of arsenic and heavy metals from mine tailings. Journal of the Taiwan Institute of Chemical Engineers, 78, 409–415.

Sukrampal, Kumar, R. and Patil, S.A. (2020). Removal of heavy metals using bioelectrochemical systems. Integrated Microbial Fuel Cells for Wastewater Treatment, 49–71.

Tian, J., Chang, H., Gao, S. and Zhang, R. (2020). How to fabricate a negatively charged NF membrane for heavy metal removal via the interfacial polymerization between PIP and TMC? Desalination, 491, 114499.

Wang, L., Wang, Y., Cui, L., Gao, J., Guo, Y. and Cheng, F. (2020). Sustainable approaches for advanced removal of iron from CFA sulfuric acid leach liquor by solvent extraction with P507. Separation and Purification Technology, 251, 117371.

Zare-Dorabei, R, Ferdowsi, S.M, Barzin, A. and Tadjarodi, A. (2016). Highly efficient simultaneous ultrasonic-assisted adsorption of Pb (II), Cd (II), Ni (II) and Cu (II) ions from aqueous solutions by graphene oxide modified with 2, 2′-dipyridylamine: central composite design optimization, Ultrason. Sonochem., 32, 265–276.

Zhang, Y., Wang, Y., Zhang, H., Li, Y., Zhang, Z. and Zhang, W. (2020). Recycling spent lithium-ion battery as adsorbents to remove aqueous heavy metals: Adsorption kinetics, isotherms, and regeneration assessment. Resources, Conservation and Recycling, 156, 104688.